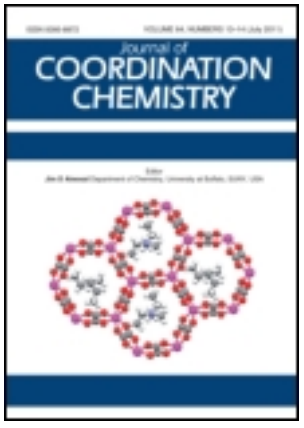

Journal of Coordination Chemistry
Publication details, including instructions for authors and subscription information:
http://www.tandfonline.com/loi/gcoo20

Synthesis, characterization, and ascorbic acid oxidase biomimetic catalytic activity of cobalt(III) oxime complexes

Abd El-Motaleb M. Ramadan [a], Shaban Y. Shaban [a] & Mohamed M. Ibrahim [a]

[a] Chemistry Department, Faculty of Science , Kafr El-Sheikh University , Kafr El-Sheikh 33516, Egypt

Published online: 23 Sep 2011.

To cite this article: Abd El-Motaleb M. Ramadan , Shaban Y. Shaban & Mohamed M. Ibrahim (2011) Synthesis, characterization, and ascorbic acid oxidase biomimetic catalytic activity of cobalt(III) oxime complexes, Journal of Coordination Chemistry, 64:19, 3376-3392, DOI: 10.1080/00958972.2011.621166

To link to this article: http://dx.doi.org/10.1080/00958972.2011.621166

Journal of Coordination Chemistry
Vol. 64, No. 19, 10 October 2011, 3376–3392

Synthesis, characterization, and ascorbic acid oxidase biomimetic catalytic activity of cobalt(III) oxime complexes

ABD EL-MOTALEB M. RAMADAN*, SHABAN Y. SHABAN and MOHAMED M. IBRAHIM

Chemistry Department, Faculty of Science, Kafr El-Sheikh University, Kafr El-Sheikh 33516, Egypt

(*Received 23 June 2011; in final form 15 August 2011*)

A new tetradentate tetraaza ligand was prepared *via* Schiff-base condensation of 3,4-diaminotoluene with 2,3-butandione monoxime in aqueous solution. This ligand coordinates cobalt(III) through nitrogen donors in equatorial positions with loss of one oxime proton with concomitant formation of an intramolecular hydrogen bond. A series of cobalt(III) complexes, $[CoLX_2]$ ($X = Cl^-$, Br^-, or I^-), [SCNCoLBr], [CNCoLBr], $[BF_2CoLBr]$, and $[YCoLBr]ClO_4$ (Y = pyridine, thiophene, triphenylphosphine, or *n*-pentylamine), was synthesized. The compounds were characterized based on the elemental analysis (C, H, N), electrical conductance, magnetic moment measurements, and spectral studies (IR, ^1H NMR, and UV-Vis). Thermal stabilities of representative complexes were examined by using thermal analysis (TGA and DTG). The reported complexes are d^6 low-spin diamagnetic and a distorted octahedral environment was proposed. All complexes undergo tetragonal distortion as evidenced by splitting of $^1T_{1g}$ and $^1T_{2g}$ levels of the pseudo-octahedral symmetry. The ligand field parameters such as Dq^E, Dq^A, and the tetragonal splitting D_t have been computed and correlated with the nature of the coordinated axial ligands. The reported cobalt(III) complexes exhibit promising catalytic activity toward aerobic oxidation of ascorbic acid to the corresponding dehydroascorbic acid. The oxidase catalytic activity is linked to both the tetragonal splitting parameter D_t and the Lewis-acidity of cobalt(III) created by the nature of the coordinated axial ligands. The probable mechanistic implications of the catalytic oxidation reactions are discussed.

Keywords: Oxime; Synthesis; Ascorbic acid oxidase; Cobalt(III); Biomimetic; Catalytic activity

1. Introduction

A number of enzymes are able to catalyze the activation of dioxygen from the atmosphere and use it in a wide variety of reactions [1, 2]. Enzymes that activate dioxygen include the oxidases, which use oxygen as an oxidant, and reduce dioxygen to hydrogen peroxide or water. One such enzyme is ascorbic acid oxidase (copper enzyme), which catalyzes the aerobic oxidation of ascorbic acid to dehydroascorbate in plants [1, 2]. Ascorbic acid is an important biological reducing agent facilitating

*Corresponding author. Email: ramadanss@hotmail.com

ISSN 0095-8972 print/ISSN 1029-0389 online © 2011 Taylor & Francis
http://dx.doi.org/10.1080/00958972.2011.621166

electron transfer in living organisms [3]. The effect of ascorbic acid on the action of enzymes is well-documented. In some cases, the effect has been activation (e.g., arginase and papain) and in others inhibitory effects (e.g., urease and β-amylase from plants). The inhibitory action of ascorbate on urease and plant β-amylase is due to reduction of Cu^{2+} to Cu^{+} [4]. Also, the redox reactions of L-ascorbic acid are of fundamental interest in chemistry, biochemistry, pharmacology, and several areas of medicine; it is necessary in human diet to synthesize collagen and epinephrine, besides preventing scurvy. The method of catalytic anticancer therapy using oxygen-centered radicals as cytotoxic agents was proposed, tested, and patented in 1995 [5]. The radicals are formed in oxidation of ascorbic acid (AH_2) with dioxygen catalyzed by phthalocyanine metal complexes. The relative catalytic activity of several substituted phthalocyanines in this reaction was estimated in 1996 [6, 7]. Further development of the method required a deeper study of the kinetics and mechanism of the reaction to establish quantitative criteria for evaluation of catalysts and recommendations on controlling the efficiency of the catalytic generation of cytotoxic agents.

Chemical models that mimic oxidases have been developed to provide the basis for understanding enzymatic activity and to develop simple catalytic systems that, under mild conditions, exhibit appreciable catalytic activity [8–15]. Synthetic model studies on the reactivity of cobalt complexes toward oxidation of ascorbic acid and phenolic substrates implicates both structural and electronic factors as being responsible for the catalytic activity [11, 12, 16].

Oximes are versatile ligands that can be bound in different ways by O and/or N and several stereoisomers are possible [17, 18]. Coordinated oxime ligands and oximate complexes display a rich variety of reactivity which leads to unusual chemical compounds [19]. Recently reviewed data show that oximes, although being classical ligands [20], display a variety of reactivity modes unusual even for modern coordination chemistry [21, 22]. The ligands and their metal complexes also played a significant role in stereochemistry, structural isomerism, spectroscopy, model systems of biochemical interest, cation exchange and ligand exchange chromatography, pigments, and dyes [23]. Dioximes are interesting for many applications in a variety of high technology fields, such as medicine [24–26], catalysis [26–28], electro, optical sensors [29], liquid crystals [30], and trace metal analysis [31].

Therefore, the structural and electronic properties of cobalt(III) oxime complexes are of interest. Synthesis, characterization, and ascorbic acid oxidase biomimetic catalytic activity of new cobalt(III) oxime complexes as functional oxidase models are the subjects of this manuscript.

2. Experimental

2.1. *Materials*

Caution: Salts of perchlorate and their metal complexes are potentially explosive and should be handled with great care and in small quantities. Cobalt salts, diacetyl monoxime (2,3-butandione monoxime), and 3,4-diaminotoluene were procured from Aldrich. All chemicals used are of high purity analytical grade.

2.2. *Preparation of the ligand*

Freshly recrystallized 3,4-diaminotoluene ($0.1\,mol\,L^{-1}$) and diacetyl monoxime ($0.2\,mol\,L^{-1}$) were dissolved in 100 mL cold water and the reaction mixture was stirred at room temperature for 30 min. Then the temperature was raised gradually and the reaction mixture was boiled under reflux with stirring for an hour, whereupon fine red solids separated. On cooling to room temperature, the solid product was removed by filtration, washed with cold methanol, and recrystallized from aqueous ethanol to give red needles (yield 75%). The purity of this ligand was checked by elemental analysis, constancy of melting point (166°C) and spectral measurements.

2.3. *Preparation of the metal chelates*

The free ligand (0.02 mol) and the cobalt salt, CoX_2 (X = Cl or Br) (0.02 mol), were dissolved in 50 cm^3 hot dry acetone. The reaction mixture was stirred vigorously for about 10 min at room temperature. The resulting fine green microcrystalline product was filtered rapidly and washed with dry acetone followed by Et_2O and finally dried under vacuum over anhydrous CaO.

The diiodo complex **3** was prepared by treating the green solution of $[CoLCl_2]$ (0.02 mol) in hot dry acetone with 2 cm^3 of saturated aqueous KI. The resulting brown solution was slowly evaporated at room temperature and a dark brown product precipitated. This brown precipitate was filtered off, washed with cold ethanol, dried in air, and then recrystallized from acetone and finally dried in vacuum over CaO.

Metathetical displacement of one of the axial bromides of the dibromo complex to obtain complexes **4** and **9** was accomplished by dissolving **2** in hot aqueous methanol and adding an aqueous solution of KX (X = SCN or CN). For the thiocyanato complex, the volume of the reaction mixture solution was reduced by slow evaporation and refrigerated at 5°C overnight. The resulting dark brown crystals were filtered and washed once with cold H_2O followed by cold ethanol and finally dried under vacuum.

For **9** the reaction mixture was refluxed for 2 h, and the volume of solution was reduced by slow evaporation on a water bath. The resulting brown solution was cooled to room temperature whereupon brown solids separated. This brown precipitate was filtered off, washed with cold water followed by dry ethanol and finally dried in air.

For **5**–**8**, to a solution of $[CoLBr_2]$ ($0.01\,mol\,L^{-1}$) in hot aqueous methanol was added two mL of a saturated aqueous solution of $NaClO_4$ followed by addition of $0.01\,mol\,L^{-1}$ of the appropriate Lewis-base (L' = pyridine, thiophene, triphenylphosphine, or *n*-pentylamine) with stirring. The resulting microcrystalline products were separated immediately by filtration, washed with cold dry methanol followed by diethyl ether, and finally dried under vacuum over CaO. Complex **10** was prepared according to the method described by Schrauzer and Windgassen [32].

2.4. *Physical measurements*

IR spectra were recorded as KBr discs from 4000 to 200 cm^{-1} on a Unicam SP-200 spectrophotometer. Electronic absorption spectra were obtained in methanol solution using a Shimadzu UV-240 spectrophotometer. ^1H NMR spectra in DMSO-d_6 were obtained on a Jeol 200 MHz NMR spectrometer. Molar conductance measurements

were carried out with a YSI Model 32 conductance meter using freshly prepared 10^{-3} molL^{-1} solutions in methanol and DMF. Magnetic susceptibility measurements were carried out by Gouy's method at room temperature. Thermogravimetric (TGA and DTG) measurements were performed using a Shimadzu TG 50-Thermogravimetric analyzer from 25°C to 800°C under N_2. The elemental analysis was carried out at the analytical unit of the Central Laboratory of Tanta University.

2.5. *Ascorbic acid oxidase catalytic studies*

The ascorbic acid oxidase catalytic activity of the cobalt(III) oxime complexes was assayed from the rate of oxidation of ascorbic acid to dehydroascorbic acid at 37°C according to the described method [33]. Dehydroascorbic acid is coupled with 2,4-dinitrophenylhydrazine (2,4-DNP) to form the 2,4-dinitrophenylhydrazone (osazone product). Treatment of the osazone with analytically pure, strong, and concentrated H_2SO_4 caused rearrangement to yield a reddish complex, which was measured at 515 nm. The concentration of the methanolic solution of cobalt(III) oxime complexes varied from 25 to 100 µmol, keeping the ascorbic acid concentration constant at 500 µmol. The blank tube contains 2,4-DNP, ascorbic acid, and distilled water.

3. Results and discussion

A new tetradentate tetraaza ligand (L) was formed *via* Schiff-base condensation of 3,4-diaminotoluene with 2,3-butanedione monoxime in 1 : 2 molar ratio in an aqueous solution. The purity and characterization of this ligand were inferred from elemental analyses and spectral measurements. The ligand provides a square planar set of nitrogen atoms and access for axial groups above and below the plane as a monoanionic ligand. The free ligand (scheme 1) is dibasic and coordinates with cobalt through its nitrogen donors in the equatorial positions with loss of one oxime proton with concomitant formation of an intramolecular hydrogen bond. Interaction of $CoCl_2$ or $CoBr_2$ with the reported ligand in acetone in the presence of atmospheric oxygen leads to the formation of 1 : 1 complex with spontaneous oxidation of cobalt(II) to cobalt(III) (scheme 1). These complexes were synthesized from cobalt(II) salts without the help of any external oxidizing agent. The ease with which cobalt(III) complexes are formed may be attributed to the ability of the reported ligand to accommodate the smaller cobalt(III) more readily than the larger cobalt(II) ion in its central cavity, in agreement with the observation of Jackels *et al.* [34] that the metal ion site in a macrocyclic ligand becomes smaller with increasing unsaturation. In the ligand under investigation, the unsaturation extends to all four donor nitrogen atoms, causing the cavity available to accommodate metal to become smaller, thereby favoring cobalt(III) over cobalt(II).

For **1**, **2**, and **3**, the two halides are coordinated to cobalt(III) in axial sites of six-coordinate complexes. Oxidation of cobalt(II) to cobalt(III) in all complexes was inferred from the magnetic moment, elemental analysis, and spectroscopic measurements. Indirect evidence for the presence of hydrogen bond in the dihalo complexes was achieved by treating **2** with boron trifluoride etherate [32], which readily reacts with the

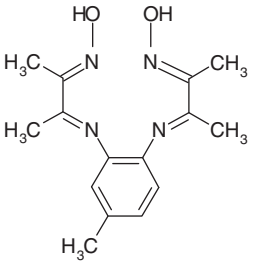

L

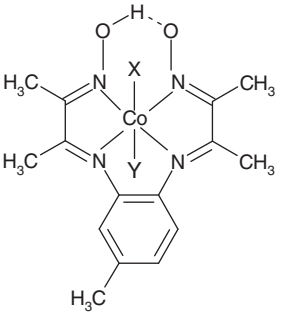

For complexes: **1**, X = Y = Br; **2**, X = Y = Cl; **3**, X = Y = I; **4**, X = Br, Y = SCN; **5**, X = Br, Y = PPh_3; **6**, X = Br, Y = pyridine; **7**, X = Br, Y = thiophene; **8**, X = Br, Y = *n*-pent; **9**, X = Br, Y = CN

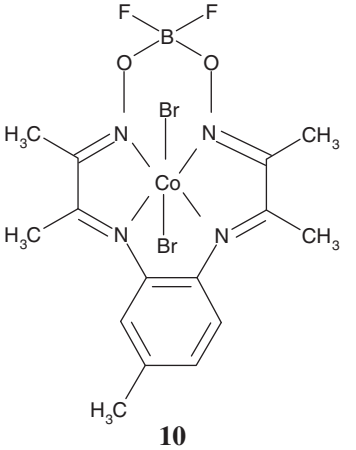

10

Scheme 1. Structure of the tetraaza ligand (L) and its cobalt(III) complexes **1**–**10**.

O–H $\cdots$ O bridge, affording an extremely stable compound containing an O–BF_2–O bridge (scheme 1).

Besides conductivity, evidence for replacement of halide by the polar solvent molecules is afforded by instantaneous precipitation of silver halide from aqueous

Table 1. Molecular formulae, elemental analyses, and physical properties of cobalt(III) oxime complexes.

Complex	Color	Λ ($\Omega^{-1}\,cm^2\,mL^{-1}$)	Found (Calcd) C	H	N
1. $[CoLCl_2]$	Green	63.7	42.9(43.37)	4.2(3.86)	13.44(13.53)
2. $[CoLBr_2]\cdot 2H_2O$	Green	78.3	33.5(33.41)	3.6(3.71)	10.18(10.40)
3. $[CoLI_2]$	Red	69.5	29.7(30.16)	3.0(2.68)	09.25(09.39)
4. [SCNCoLBr]	Brown	90.3	39.53(39.84)	3.5(3.32)	13.95(14.53)
5. $[L'CoLBr]ClO_4$	Faint brown	78.5	49.98(50.42)	4.3(3.95)	06.85(07.13)
6. $[L'CoLBr]ClO_4$	Light brown	77.4	39.56(39.90)	3.62(3.49)	11.21(11.64)
7. $[L'CoLBr]ClO_4$	Greenish-brown	76.5	37.42(37.60)	4.10(3.29)	08.78(09.24)
8. $[L'CoLBr]ClO_4$	Dark brown	90.2	39.17(39.38)	4.4(5.75)	10.97(11.49)
9. [CNCoLBr]	Brown	–	42.55(42.77)	3.33(3.56)	15.49(15.60)
10. $[BF_2CoLBr_2]\cdot 2H_2O$	Dark brown	–	30.92(30.82)	3.12(3.42)	09.20(09.59)

For **5**, L′ = triphenylphosphine; **6**, L′ = pyridine; **7**, L′ = thiophene; **8**, L′ = *n*-pentylamine.

alcoholic solution of the complexes by silver nitrate. In aqueous methanolic solution of the dichloro and dibromo complexes, the brown transparent solutions gave the original green precipitates upon addition of hydrochloric or hydrobromic acid. This illustrates that in aqueous solution the axially coordinated halides are reversibly replaced by water.

All the complexes (except **9** and **10**) are soluble in DMF and partially soluble in water, methanol, and aqueous methanol. Solubility was enhanced by ultrasonic bath. The molar conductivities of the investigated complexes in DMF fall in the range 63.7–90.3 $\Omega^{-1}\,cm^2\,mol^{-1}$, showing that they are 1 : 1 electrolytes [35] with one halide replaced by DMF. Formation of [LCo(III)XDMF]X was confirmed from the fact that, in pure methanol, the complexes are nonelectrolyte with molar conductivities of 28.3–31.0 $\Omega^{-1}\,cm^2\,mol^{-1}$, indicating little solvent substitution for the axial ligands. It is difficult to measure the molar conductances of **9** and **10** because they are only partially soluble in DMF and completely insoluble in other organic solvents and water. The pure compounds are listed in table 1 together with their analytical data and some physical properties. Elemental analyses are in reasonable agreement with the proposed structures in scheme 1. The reported complexes are various shades of green and brown and are crystalline or microcrystalline powders, stable as solid or in the solution under atmospheric conditions.

3.1. *IR spectra*

IR spectrum of the free ligand shows no characteristic absorptions assignable to either a C=O or NH_2 function, confirming the formation of the Schiff base. The strong, sharp band at 1512 cm^{-1} is assigned to υ(C=N) and oxime linkages [36, 37], whereas the other strong sharp band at 1200 cm^{-1} is due to υ(N–O) [36, 37]. The strong band of medium broadness at 1460 cm^{-1} and the weak band at 1410 cm^{-1} are assigned to ring modes of ortho-disubstituted toluene [37]. Sharp bands of medium intensity at 1370 and 1440 cm^{-1} are due to symmetric and asymmetric deformation vibrations, respectively, of the methyl groups [36]. Strong sharp bands at 1255, 1165 and 1120 cm^{-1} are assigned to υ(C–C), υ(C–N), or the coupled vibration between these modes. The metal-sensitive

strong and sharp band at 760 cm^{-1} may be attributed to C=N–O deformation. The metal-dependent strong and sharp bands at 975, 910, and 895 cm^{-1} can be ascribed to deformation modes of the ligand [38].

The characteristic IR absorptions of the ligand are shifted and decreased in intensity on complex formation and new vibrational bands appear. Vibrational evidence for N-coordination of the oximato group (five-membered chelate ring) in all complexes is provided by the higher frequency of υ(N–O) at *ca* 1200–1220 cm^{-1} [39]. Consequently, υ(N–O) is expected to have greater double bond character than the corresponding υ(N–O) of oximino–oxygen coordination. Coordination of the azomethine nitrogen to cobalt reduces the υ(C=N) frequency by 7–27 cm^{-1} compared to free ligand. A broad band of medium intensity at 2846–2900 cm^{-1} in the free ligand shifts to 2330–2362 cm^{-1} on complex formation, attributed to υ(OH) of the hydrogen bond (O–H $\cdots$ O) [36b, 40]. The IR spectrum of **10** resembles that of **2** except for new bands characteristic of BF_2 group and the absence of υ(OH) and υ(N–O) bands. The weak band at 1695 cm^{-1} belonging to O–H $\cdots$ O bending disappears upon formation of the boron-bridged complex with concomitant appearance of peaks due to the BF_2 bridge. The weak band at 1175 cm^{-1} and the strong sharp band at 826 cm^{-1} are ascribed to B–O stretching modes while weak bands at 1026 and 1006 cm^{-1} are attributed to B–F stretches of the BF_2 derivatives [41].

The spectrum of the thiocyanato complex **4** exhibits absorptions at 2050 cm^{-1} υ(SCN), 815 cm^{-1} υ(CNS), and a medium band at 480 cm^{-1} υ(NCS), characteristic of monodentate N-bonded thiocyanate [42]. This is further confirmed by the appearance of a new absorption at 280 cm^{-1}, which is characteristic of (M–NCS) [43]. The cyano-complex exhibits a strong absorption band at 2160 cm^{-1} for υ(CN) and a weak band of medium broadness at 440 cm^{-1} assignable to υ(Co–C) [42].

All complexes containing perchlorate have expected υ_3 and υ_4 bands with T_d-symmetry without splitting at 1083–1089 and 629–649 cm^{-1}, clearly revealing that ClO_4^- does not coordinate to cobalt(III) [44]. The sharp and strong band at 629–649 cm^{-1} indicates ionic ClO_4 [42]. The coordinated Lewis bases pyridine, thiophene, triphenylphosphine, and *n*-pentylamine exhibit υ(CH) at 2960–3034 cm^{-1} and the coupled υ(C=C) vibrations around 1631 and 1600 cm^{-1}. Spectra of the coordinated *n*-pentylamine exhibit υ(CH) in the region 2960–3034 cm^{-1} and vibrations of PPh_3 at 1631 cm^{-1}. The υ(C=N) and υ(C–S) frequencies of the pyridine ring and thiophene appear at 1557 cm^{-1} and 833 cm^{-1}, respectively; υ(CH) deformation, in plane ring deformation, and out of plane ring deformation of pyridine are at 762, 705, and 416 cm^{-1}.

In all complexes the metal–nitrogen stretching vibration υ(Co–N) occurs at 507–519 cm^{-1} [42]. Far IR spectra exhibit absorption at 308–384 cm^{-1}, associated with coordinated halide [42, 45]. The antisymmetric and symmetric OH stretching of lattice water appear at 3423–2460 cm^{-1} in spectra of **2** and **10**, in addition to another absorption at 410–360 cm^{-1} characteristic of lattice water [42, 46]. The IR spectral data of the reported compounds are given in table 2.

3.2. *^{1}H NMR spectra*

Magnetic moment measurements demonstrated that the synthesized cobalt complexes are diamagnetic, indicating cobalt(III). This enables us to further confirm structures by

Table 2. Characteristic IR spectral bands of L and its cobalt(III) oxime complexes.

Compound[a]	υ(O–H···H)	υ(C=N)	υ(NO)	υ(M–N)	υ(M–X)
L	2846[b]	1512	1200	–	–
1	2337	1495	1228	513	384
2	2362	1485	1218	511	376
3	2335	1500	1221	513	381
4	2360	1485	1220	517	375
5	2339	1490	1242	519	375
6	2362	1490	1237	511	356
7	2337	1495	1230	507	326
8	2330	1480	1237	513	326
9	2357	1490	1220	511	318
10	–	1485	1218	511	370

[a]Complex details are as listed in Table 1.
[b]This band is assigned to the υ(OH) of the free ligand.

employing ^{1}H NMR. The ^{1}H NMR spectral data are listed in table 3. The three types of methyls are inequivalent in the present ligand and its complexes. These spectral data provide insight regarding the structures of the reported complexes. The three resonances at $\delta = 1.93$ (6H), 2.65 (6H), and 3.29 (3H) ppm in the spectrum of free ligand were shifted downfield when the ligand coordinated to cobalt(III). For example, they appear at $\delta = 2.35$, 2.39, and 2.65 ppm in **2**. The aromatic protons appear as three multiplets at 7.56, 7.73, and 7.81 ppm in the free ligand and shift upfield when ligated to cobalt(III). A characteristic broad peak in the free ligand at $\delta = 11.31$ ppm, exchanged by D_2O, is assigned for two protons of the oxime. This peak cannot be seen in the spectra of the complexes, suggesting deprotonation of the OH when the ligand coordinates to cobalt(III). Figure S1 depicts the 200 MHz ^{1}H NMR spectrum of **2** together with the ligand L.

3.3. *Electronic absorption spectra*

Octahedral low-spin d^6 cobalt(III) complexes are spin paired and diamagnetic. Two principal spin-allowed absorption bands are to be expected for transition from the $^1A_{1g}$ ground state to the $^1T_{1g}$ and $^1T_{2g}$ excited states in the octahedral environment O_h [47]. On descent in symmetry to D_{4h} or C_{4v}, corresponding to the tetragonal distortion, the degeneracy of the octahedral $^1T_{1g}$ and $^1T_{2g}$ levels is removed. When the symmetry is lowered from O_h to D_{4h}, the $^1A_{1g} \rightarrow {}^1T_{1g}$ splits into two bands, $^1A_{1g} \rightarrow {}^1E_g$ and $^1A_{1g} \rightarrow {}^1A_{2g}$, and the second band, $^1A_{1g} \rightarrow {}^1T_{2g}$, splits into $^1A_{1g} \rightarrow {}^1E_g^*$ and $^1A_{1g} \rightarrow {}^1B_{2g}$ (the higher energy $^1E_g^*$ level has an asterisk to distinguish it from the low energy ^1E_g level). Thus when the symmetry is lowered to D_{4h}, more than two bands are expected, usually three, assigned to $^1A_{1g} \rightarrow {}^1E_g$, $^1A_{1g} \rightarrow {}^1A_{2g}$ and $^1A_{1g} \rightarrow ({}^1B_{2g} + {}^1E_g^*)$. The splitting of the latter band namely $^1A_{1g} \rightarrow ({}^1B_{2g} + E_g^*)$ has never been observed experimentally, probably due to the onset of the charge-transfer bands or due to the ligand field [48]. The splitting of the first excited state $^1T_{1g}$ of the octahedral geometry in a D_{4h} or C_{4v} symmetry is associated with a single tetragonal splitting parameter D_t. If the in-plane field strength is greater than the out-of-plane field strength then D_t will be positive and the ^1E_g level will lie lower than $^1A_{2g}$. The splitting of the $^1T_{1g}$ becomes

Table 3. ^{1}H NMR spectral data (δ, ppm) of L and its cobalt(III) oxime complexes.

Compound	CH_3 (15 H)	Ar–CH_3	Aromatic protons	OH
L	1.93, 2.65	3.29	7.557, 7.728, 7.811	11.313
1	2.35, 2.65	4.19	7.418, 7.588, 7.697	–
2	2.31, 2.60	4.08	7.475, 7.611, 7.741	–
3	2.28, 2.38	3.93	7.383, 7.562, 7.655	–

Complex details are as listed in Table 1.

larger as the difference in the ligand field strength between the in-plane (equatorial plane) and out-of-plane (axial plane) increases.

To interpret the electronic absorption spectra and to compute the ligand field strength, the D_{4h} symmetry has been assumed for the cobalt(III) complexes. Computation of the ligand field strength of the equatorial ligands (Dq^E), and that of the axial ligands (Dq^A), was achieved by using the following equations [49]:

$$^1A_{1g} \rightarrow {}^1A_{2g} = 10Dq^E - C, \tag{1}$$

$$^1A_{1g} \rightarrow {}^1E_g = 10Dq^E - C - 35/4\,D_t, \tag{2}$$

$$Dq^A = Dq^E - 7/4\,D_t. \tag{3}$$

The interelectronic repulsion parameter C is taken to be 3800 cm^{-1} and this value is given by Wentworth and Piper [48] to be roughly independent of field strength. The electronic spectral band assignments and the ligand field parameters for the reported complexes are given in table 4. The dihalo [$CoLX_2$] and the pseudo-halogeno [SCNCoLBr] complexes exhibit three absorptions at 17,544–18,377, 22,137–23,839 and 25,839–27,777 cm^{-1}. The occurrence of these bands in the visible region is characteristic of tetragonally distorted cobalt(III) complexes [50]. These bands are assigned to $^1A_{1g} \rightarrow {}^1E_g$, $^1A_{1g} \rightarrow {}^1A_{2g}$ and $^1A_{1g} \rightarrow ({}^1B_{2g} + {}^1E_g^*)$ transitions, respectively. The ligand field parameters Dq^E, Dq^A, and the single tetragonal splitting parameter D_t were calculated based on these band assignments (table 4). The energy of $^1A_{1g} \rightarrow {}^1A_{2g}$ transition and the values of D_t and Dq^A show a dependence on the nature of the coordinated axial ligands and follow the order SCN > Cl > Br > I, in good agreement with the positions of these ligands in the spectrochemical series. This order (SCN > Cl > Br > I) reflects that, as the ligand field strength of the axial ligands increases, the out-of-plane field strength also increases. Accordingly, the splitting of the first excited state $^1T_{1g}$ becomes larger and consequently the values of the single tetragonal splitting parameter D_t increases with increase in the field strength of the axial plane (i.e. Dq^A). A similar spectral behavior was observed for analogous six-coordinate d^6 cobalt(III) complexes [48, 51]. It has been previously reported that the value of D_t is directly proportional to the extent of the tetragonal distortion in D_{4h} symmetry [49]. The data in table 4 reveal that the values of the single tetragonal splitting parameter D_t of **1**–**4** increases in the order **4** > **1** > **2** > **3**.

The spectrum of the cyano complex shows two absorptions at 18,735 and 27,397 cm^{-1} assignable to $^1A_{1g} \rightarrow {}^1T_{1g}$ and $^1A_{1g} \rightarrow {}^1T_{2g}$, respectively, in pseudo-octahedral symmetry O_h [52]. Consequently, the ligand field parameters Dq^E, Dq^A, and

Table 4. Electronic spectral assignments and ligand field parameters (cm^{-1}) of cobalt(III) oxime complexes **1**–**9**.

Complex	$^1A_{1g} \rightarrow {}^1E_g^*$	$^1A_{1g} \rightarrow {}^1A_{2g}$	$^1A_{1g} \rightarrow ({}^1E_g + {}^1B_{2g})$	Dq^E	Dq^A	D_t
1	17,887	23,230	25,839	2703	1635	610
2	17,544	22,727	27,027	2652	1616	592
3	17,135	22,137	27,397	2593	1593	571
4	18,377	23,989	27,777	2778	1656	641
5	17,833	23,155	26,666	2695	1631	608
6	17,787	22,996	26,525	2679	1638	595
7	17,824	23,238	26,809	2692	1633	605
8	18,165	23,567	27,562	2736	1656	617
9	17,767	–	27,397	–	–	–

Complex details are as listed in Table 1.

the single tetragonal splitting parameter D_t cannot be computed. The Lewis-base complexes (**5**–**8**) exhibit three absorptions as does **2**. This leads to D_t values 608, 595, 605, and 617 cm^{-1} for **5**, **6**, **7**, and **8**, respectively. The lone-pair electron density on the primary nitrogen of *n*-pentylamine is higher than that on the pyridine nitrogen; therefore, the axial field strength (Dq^A) of pyridine is lower than that of *n*-pentylamine. Consequently, the D_t value and the extent of tetragonal distortion of **8** is greater than that of **6**. Although the axial field strength (Dq^A) of coordinated pyridine (1638 cm^{-1}) is higher than that of triphenylphosphine (1631 cm^{-1}) and thiophene (1633 cm^{-1}), it is surprising that the tetragonal splitting parameter D_t caused by pyridine is 595 cm^{-1} as against 608 cm^{-1} and 605 cm^{-1} for the triphenylphosphine and thiophene, respectively, contrary to the observation that the tetragonal splitting is higher when the field strength of the axial ligand is higher. This unusual behavior can be rationalized by correlation between the extent of tetragonal distortion of these complexes and the effect of the "*entatic state*" [53]. According to the hypothesis of "*entatic state*", any small changes in symmetry of the coordination environment of the metal ion are usually associated with an increase in the degree of symmetry distortion [54]. For octahedral **5**, **6**, and **7**, the coordination chromospheres are [CoNNNNPBr], [CoNNNNNBr], and [CoNNNNSBr], respectively. Greater static distortion must be expected in **5** and **7** because their coordination environments contain two nonidentical donating atoms. On the other hand, there is only one nonidentical donating atom in **6**.

3.4. *Thermogravimetric analysis (TGA and DTG)*

The content of a particular component can be determined based on the mass losses of these components in thermogravimetric plots [55]. Therefore, TG and DTG techniques were performed. The TG and DTG thermograms of representative complexes were recorded under a dynamic N_2 atmosphere and some important characteristics are listed in table 5. The TG curve was redrawn as mg mass loss *versus* temperature.

The TG plots of **1**, **3**, **4,** and **10** are similar and showed that they decomposed in three successive overlapped and unresolved steps, occurring from 100°C to 650°C with a net weight loss of 78.51–91.54%. The percentage weight losses were consistent with the elimination of the coordinated counter anions and the organic ligand (table 5).

Table 5. Thermogravimetric analysis data of cobalt(III) oxime complexes.

Complex	Temperature range (°C)	DTG T (°C)	Weight loss Found (Calcd)	Species formed
1	120–220	190	08.37(08.51)	CoLCl
	220–400	340	21.91(22.28)	$CoL_{(0.8)}$
	400–600	530	48.60(49.38)	Co_2O_3
2	100–140	110	06.51(06.64)	$CoLBr_2$
	140–410	390	29.92(29.49)	CoL
	410–610	550	35.27(35.28)	$CoL_{(0.275)}$
	610–730	685	12.98(13.38)	Co_2O_3
3	160–220	195	21.21(21.15)	CoLI
	220–290	260	33.49(32.64)	$CoL_{(0.76)}$
	290–600	550	36.84(36.37)	Co_2O_3
4	150–270	240	11.97(11.89)	CoLBr
	270–350	320	16.23(16.51)	CoL
	350–600	535	58.86(59.31)	Co_2O_3
10	100–140	110	06.57(06.16)	$CoLBr_2 \cdot BF_2$
	140–300	235	13.51(13.32)	$CoLBr \cdot BF_2$
	300–650	525	64.84(65.60)	Co_2O_3

Complex details are as listed in Table 1.

For **1**, **3**, **4,** and **10**, the first stage of decomposition starts at 100 and ends at 270°C with mass losses (6.57–21.21%) due to partial elimination of the coordinated halide and thiocyanate, in agreement with the calculate masses of 6.00–21.15%. The maximum rate of mass loss occurs at 150°C as indicated by the DTG peak.

The second stage starts at 140°C and ends at 410°C with a DTG peak at 250°C. The corresponding mass losses (13.51–33.49%) are attributed to complete elimination of the coordinated anions in addition to partial decomposition of the organic moiety. The third stage starts at 300°C and comes to end at 650°C with DTG peak at 550°C. The corresponding weight losses (36.84–64.84%) are due to complete decomposition of the remaining organic portion in the complex molecule. The mass losses in the second and the third stages are in agreement with the calculated mass loss values and the final residue is quantitatively proved to be anhydrous metal oxide (Co_2O_3).

The thermogram of **2** showed that it decomposed in four successive overlapped steps from 100°C to 730°C. $CoLBr_2 \cdot 2H_2O$ complex was thermally stable to 60°C and its thermal decomposition started at this temperature. The first decomposition step occurred at 100°C and the observed mass loss (6.51%) is due to removal of two surface water molecules. The second stage of mass loss reveals that the anhydrous bromo complex is then dehalogenated at 120–410°C, with DTG maximum at 390°C. This process corresponds to volatilization of the coordinated bromides. The third and fourth stages involve a significant mass loss from 410°C to 730°C with DTG maximum peaks at 550°C and 685°C corresponding to complete decomposition of the organic ligand in successive steps, leaving behind cobalt(III) oxide. The activation energy values are 138.46 and 36.96 kJ mol^{-1} for the third and fourth stages, respectively.

3.5. *Ascorbic acid oxidase catalytic activity*

The two-electron oxidation of ascorbic acid to dehydroascorbic acid was investigated because this is one of the reactions that oxidase enzymes catalyze [2–4]. The oxidase

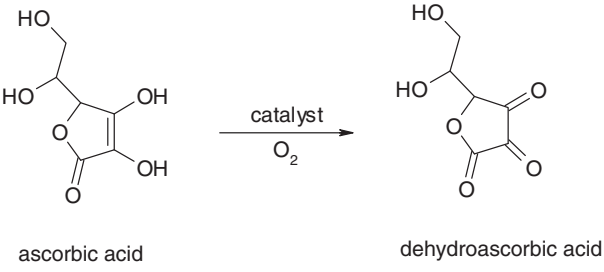

Scheme 2. Catalytic aerobic oxidation of L-ascorbic acid to the dehydroascorbic acid.

catalytic activities of the synthesized cobalt(III) oxime complexes were investigated for aerobic oxidation of vitamin C to the corresponding dehydroascorbic acid (scheme 2). The oxidase catalytic activity was evaluated from the relation: [% Oxidase catalytic activity $= (\Delta_1 - \Delta_2)/\Delta_1 \times 100$], where Δ_1 and Δ_2 are the optical densities of the sample (in presence of complex) and the control (in the absence of the complex), respectively, at 515 nm. From the results given in table 6, it is obvious that complexes **1–8** catalyze the aerobic oxidation of ascorbic acid to the corresponding dehydroascorbic acid and two molecules of water as a by-product. Complexes **9** and **10** lack sufficient solubility to study. Table 6 reports the oxidase catalytic activity of each complex, giving its final concentration that produces efficient oxidase catalytic activity.

There are two factors to consider in explaining the differences in catalytic reactivates of **1–8**: (i) the geometry imposed by the ligands on cobalt(III) and (ii) the basicity of the coordinated axial ligands in the complex and their influence on the Lewis acidity of the central cobalt(III).

3.5.1. Geometrical considerations. The data in table 6 show that ascorbic acid oxidase catalytic activity is strongly dependent on the nature of the coordinated axial ligands. The reactivity of the complexes follows the order $\mathbf{8} > \mathbf{7} \geq \mathbf{5} > \mathbf{6} > \mathbf{4} > \mathbf{1} > \mathbf{2} > \mathbf{3}$. Although **1–8** have octahedral geometry, the coordination environment varies from one complex to the other. The degree of coordination irregularity is dependent on the nature of the axial ligands attached to cobalt(III). According to the *entatic* hypothesis [53], any small changes in irregularity (symmetry) of the coordination geometry of the metal ion are usually associated with enhancement in catalytic efficiency. Vallee and Williams [54] rationalized this fact with their theory of the "*entatic state*" of a catalytically active enzyme.

As shown from the spectroscopic results, tetragonal distortion of the investigated complexes is expressed in terms of D_t (cm^{-1}) and increases in the order $\mathbf{4} > \mathbf{8} > \mathbf{5} > \mathbf{7} > \mathbf{1} > \mathbf{6} > \mathbf{2} > \mathbf{3}$. Therefore, for the halogeno and thiocyanato complexes the catalytic activity is in good agreement with the order of the tetragonal splitting parameter D_t of these pseudo-octahedral chelates. This means that the actual distortion of the metal coordination environment is the key factor of the catalytic reactivity of these halogeno and thicyanato cobalt(III) oxime oxidase models toward the aerobic oxidation of ascorbic acid.

Table 6. Oxidase catalytic activity of cobalt(III) oxime complexes **1**–**8**.

Complex	[Cat] (μmol)	Oxidase catalytic activity (%)
1	25	40 ± 1
	50	49 ± 1
	100	65 ± 2
2	25	36 ± 1
	50	47 ± 2
	100	59 ± 3
3	25	29 ± 1
	50	37 ± 1
	100	46 ± 1
4	25	43 ± 1
	50	57 ± 2
	100	72 ± 2
5	25	50 ± 1
	50	59 ± 1
	100	75 ± 3
6	25	41 ± 1
	50	53 ± 2
	100	67 ± 1
7	25	50 ± 1
	50	57 ± 2
	100	77 ± 2
8	25	60 ± 1
	50	67 ± 2
	100	90 ± 3

Complex details are as listed in Table 1.

3.5.2. The basicity of the coordinated axial ligands. The data in table 6 reveal that, for a given complex, [$CoLBr_2$] coordination of Lewis-base to cobalt(III) increases the strength of the axial ligand field and consequently increases the tetragonal splitting parameter values, in agreement with the degree of irregularity of coordination geometry increasing the catalytic activity of the corresponding catalyst [56]. Although the cobalt(III) center in **2** has a tetragonal splitting parameter D_t value close to that of **6**, the latter exhibits higher oxidase activity. Complexes **5**, **6**, **7,** and **8** have D_t values lower than the thiocyanato complex **4** (table 6), but the latter exhibits lower oxidase catalytic activity, contrary to the observation that the catalytic activity would be higher when the tetragonal splitting is higher. The difference in catalytic activity cannot be attributed only to the degree of tetragonal distortion of cobalt(III) of these complexes, but the *trans-influence* and *trans-effect* of the axially coordinated Lewis-base must also be considered [56].

Although **1**–**8** are coordinately saturated, they have at least one coordination site occupied by a good leaving group X (X = SCN or halogen donor). A ligand X frequently must be dissociated to make a coordination site available for binding ascorbic acid (H_2A), O_2 or any reacting species during catalytic oxidation, and the important factor then is the strength of the metal-X bond itself. Coordination of Lewis-base, which is a better electron donor than X, reduces the positive charge on the

cobalt(III) weakening bonding between the metal ion and all other ligands. The effect is more pronounced for ligand in the *trans* position to Lewis-base (*trans influence*) [56]. As a consequence of the bond weakening of the octahedral cobalt(III) complex or any octahedral species formed during the catalytic cycle, the activation energy of an exchange process may be lowered by destabilization of the ground state of the initial complex or by stabilization of the transition state (*trans effect*) [57]. Thus, the binding of ascorbic acid (AH_2) to cobalt(III) can occur more easily, with displacement of the labile bromide ligand as shown in the following equation:

$$2[L'CoLBr] \rightleftharpoons 2Br^- + 2[L'CoL]^+ + H_2A \rightarrow [(L'Co)_2A] + 2HBr.$$

Also, coordination of Lewis-base (L′) to the central cobalt(III) ion may change the electronic structure of the whole complex and the bond weakening in the complex will reduce the build up of the electron density on cobalt. This may reduce the redox potential of the couple Co^{III}/Co^{II} during the catalytic sequence (scheme 3).

Additional effect of the Lewis-base coordination on the rate determining step(s) of the catalytic cycle could be simplified as follows. Excessive bond stability of a metal-substrate or any reacting species is unfavorable for the catalytic process. The bond must be stable enough to exist but susceptible to reaction. Thus, the stronger the donor property of the axial Lewis-base, the stronger is the destabilization of the metal-substrate bond.

3.5.3. Suggested mechanism for the catalytic oxidation of ascorbic acid. The possible mechanistic implications (scheme 3), whereby cobalt(III) oxime oxidase models catalyze the aerobic oxidation of ascorbic acid (H_2A) to dehydroascorbic acid, imply the following interactions: (i) Owing to the lability of the halide (X) in the six-coordinate complex [$CoLX_2$], exchange interaction between the more basic ascorbate (A^{2-}) with X is expected to occur, forming the dicobalt(III)-ascorbate intermediate; such intermediate is well-known in oxidase models. (ii) As a consequence of this interaction, electron transfer from A^{2-} to two cobalt(III) ions occurs and produces two cobalt(II) centers in addition to dehydroascorbic acid.

At this stage, for Lewis-base species, $[L'Co^{II}L]^+$, the resulting five-coordinate complex is unstable in its ground state due to: (i) excessive build up of electron density on the central cobalt(II), and (ii) the tetrahedral preference of cobalt(II) [47, 49]. Consequently, we suggest that axially coordinated Lewis-base could dissociate from the five-coordinate complex and the coordination number decreases from five to four. Such conformational changes provide one open site for coordination to any reacting species during the catalytic cycle. (iii) Irreversible reaction of the cobalt(II) complex with O_2 gives *cis* – μ–η^1: η^1 or a–μ–η^2: η^2 peroxide adducts $[(LCo^{III}X)_2O_2]$ and $[(LCo^{III})_2O_2]$. This process presumably involves the transfer of an electron from cobalt(II) to oxygen, as $[(LCo^{III}X)_2O_2]$ and $[(LCo^{III})_2O_2]$ complexes react more readily with ascorbate than $[LCo^{II}X]$ and $[LCo^{II}]$ species, according to the electroneutrality principle [58]. Previous studies [59] involving metal complexes catalyzing analogous oxidations suggested formation of the dimeric species, in the rate determining step. Accordingly, the initiation step almost certainly involves production of cobalt(II) by interaction of cobalt(III) with AH_2. In this situation the Co^{II}/Co^{III} couple is involved as a redox center. (iv) Exchange interactions between the more basic and highly reactive ascorbate A^{2-} with the good leaving group X of $[(XLCo^{III})_2O_2]$ lead to the formation of

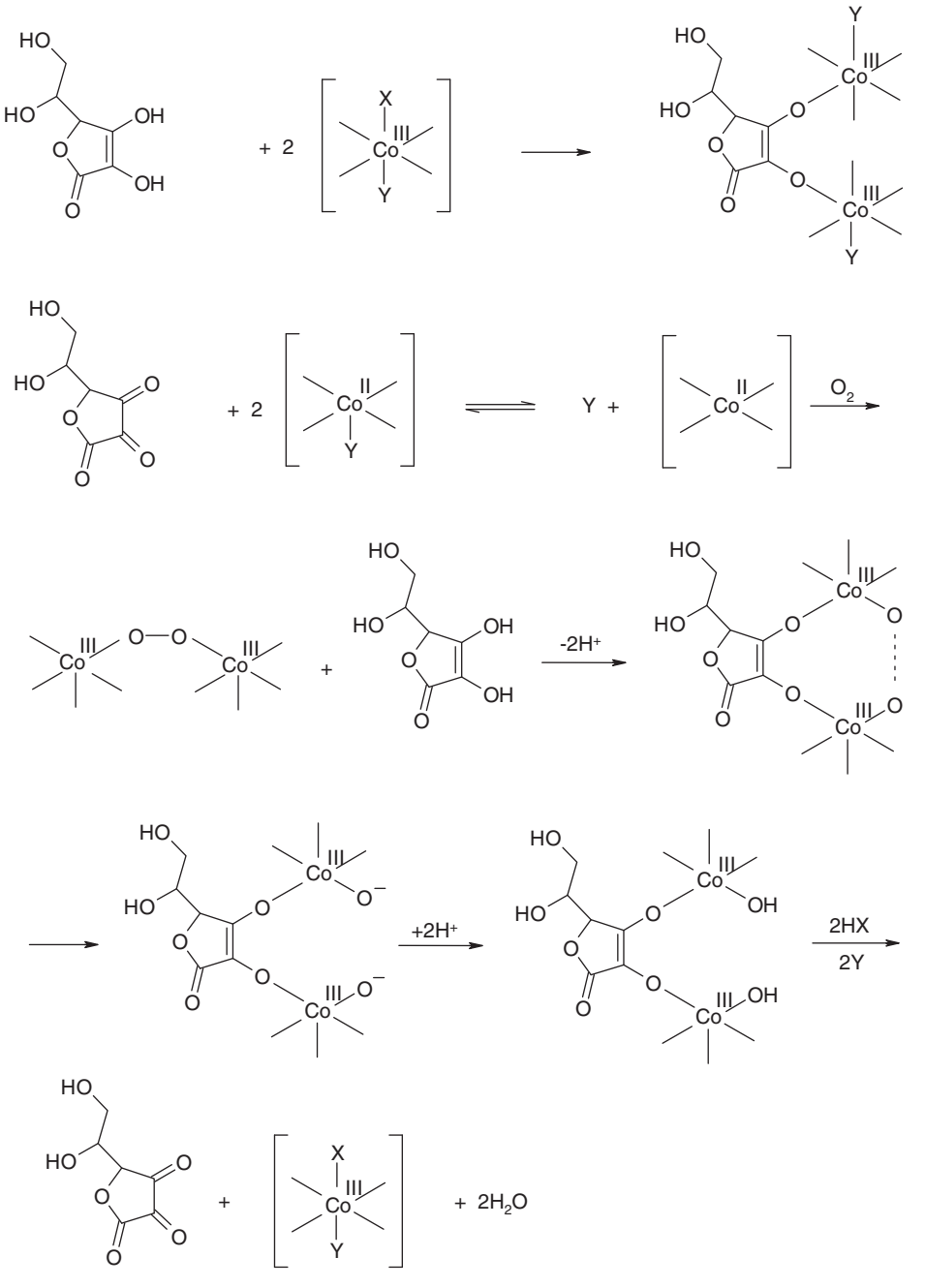

Scheme 3. The possible mechanism whereby cobalt(III) oxime oxidase models catalyze the aerobic oxidation of ascorbic acid to the dehydroascorbic acid.

$[A(LCo^{III})_2O_2]$. For the generated five-coordinate complex, $[(LCo^{III})_2O_2]$, a fast direct attack of A^{2-} on the free axial position of cobalt(III) is expected due to octahedral preference of cobalt(III) [47, 49]. As a consequence of these interactions, $[A(LCo^{III})_2O_2]$

undergoes rearrangement to give an oxide, which remains coordinated to the cobalt(III) center. The protonation of O^{2-} prior to its release from complex is required, because the oxide is highly basic and too unstable to be released in its unprotonated form. Thus, we suggest that the oxide fragment rearranges to the hydroxide radical (HO^-) as a result of electrophilic attack by a proton on the highly basic oxide bound to cobalt(III) providing the HO^- radical. (v) Finally, this intermediate could be recognized under further electrophilic attack by a proton on the highly basic hydroxide anion bound to cobalt(III) to the totally oxidized dehydroascorbic acid and two water molecules as a by-product and regeneration of the catalyst in its original active form (scheme 3).

4. Conclusion

In this study we synthesized a new tetradentate tetraaza ligand *via* Schiff-base condensation of 3,4-diaminotoluene with 2,3-butandione monoxime in water. A series of cobalt(III) complexes containing the reported ligand and various anions and Lewis bases in the axial positions have been isolated. Single crystals of the complexes could not be isolated from any solutions. However, the analytical, magnetic, conductance data, and the spectroscopic measurements enable us to propose an octahedral structure with all complexes undergoing tetragonal distortion. The tetragonal splitting parameter D_t has been computed from the spectral data and correlated with the nature of the coordinated axial ligands. The ability of complexes to oxidize ascorbic acid to dehydroascorbic acid show that the oxidase catalytic activity is strongly dependent on the nature of the coordinated axial ligands. The mechanistic implications of the catalytic aerobic oxidation of ascorbic acid are discussed.

References

[1] T.D.H. Bugg. *Tetrahedron*, **59**, 7075 (2003).
[2] T.D.H. Bugg. *An Introduction to Enzyme and Coenzyme Chemistry*, 1st Edn, Chap. 3, Blackwell Science, Oxford (1997).
[3] W. Kaim, B. Schwederski. *Bioinorganic Chemistry: Inorganic Elements in Chemistry of Life*, Chap. 5, Wiley, New York (1995).
[4] J. Reedijk., *Bioinorganic Catalysis*, Chaps 11, 13, Marcel Dekker, New York (1993) and references therein.
[5] Patent RF No. 2106, 1997, US Pat. 6, 004, 953, Dec. 21 (1999).
[6] M.E. Volpin, N. Yu. Krainova, I.V. Moskaleva, G.N. Novodarova, G.N. Vorozhtsov, M.G. Galpern, O.L. Kaliya, E.A. Lukyanets, S.A. Mikhalenko. *Izv. Akad. Nauk, Ser. Khim.*, **44**, 2105 (1996).
[7] M.E. Volpin, N.Y. Krainova, I.V. Moskaleva, G.N. Novodarova, G.N. Vorozhtsov, M.G. Galpern, O.L. Kaliya, E.A. Lukyanets, S.A. Mikhalenko. *Russ. Chem. Bull., Int. Ed.*, **45**, 1996 (2000).
[8] R. Jorge, K. Bernt. *J. Chem. Soc., Dalton Trans.*, **20**, 3793 (1997).
[9] O. Seneque, M. Campion, B. Douziech, M. Giorgi, E. Riviere, Y. Journaux, Y. Le Mest, O. Reinaud. *Eur. J. Inorg. Chem.*, 2007 (2002).
[10] S. Lakshmi, D. Saravan, R. Renganathan, M. Velusamy. *J. Inorg. Biochem.*, **61**, 155 (1996).
[11] H.D. Moya, N. Coichev. *J. Braz. Chem. Soc.*, **17**, 364 (2006).
[12] E.G. Girenko, S.A. Borisenkova, O.L. Kaliya. *Russ. Chem. Bull., Int. Ed.*, **51**, 1236 (2002).
[13] A.M. Ramadan, I.M. El-Mehasseb. *Transition Met. Chem.*, **23**, 183 (1998).
[14] M. Hassanein, S. Gerges, M. Abdo, S. El-Khalafy. *J. Mol. Catal.*, **240**, 22 (2005).
[15] A.M. Ramadan, I.M. El-Mehasseb, R.M. Issa. *Transition Met. Chem.*, **31**, 730 (2006).

[16] (a) L.I. Simandi, T. Barna, G. Argay, T.L. Simandi. *Inorg. Chem.*, **34**, 6337 (1995); (b) O.S. Jung, C.G. Pierpont. *Inorg. Chem.*, **33**, 2227 (1994); (c) L.I. Simandi, T.M. Simandi, Z. May, G. Besenyei. *Coord. Chem. Rev.*, **245**, 85 (2003); (d) J. Qiu, Z. Liao, X. Meng, L. Zhu, Z. Wang, K. Yu. *Polyhedron*, **24**, 1617 (2005); (e) D. Kovala-Demertzi, S.K. Hadjikakaou, M.A. Demertzis, Y. Deligiannakis. *J. Inorg. Biochem.*, **69**, 223 (1998); (f) J.H. Yang, G.S. Vigee. *J. Inorg. Biochem.*, **41**, 7 (1991).
[17] S.T. Malinovskii, B. Coropceanu, O.A. Bologa, A.P. Rija, M. Gdaniec. *J. Struct. Chem.*, **48**, 506 (2007).
[18] S. Serin. *Transition Met. Chem.*, **26**, 300 (2001).
[19] Z. Bologa. *Crystallogr. Rep.*, **47**, 51 (2002).
[20] P. Bourosh, I. Bulhac, Y.A. Simonov, M. Gdaniec, K. Turta, L. Siretsanu. *Russ. J. Inorg. Chem.*, **51**, 1202 (2006).
[21] M. Sahin, N.K. Cak, H.I.U. Can, M.A. Deveci. *Russ. J. Coord. Chem.*, **33**, 680 (2007).
[22] Y.Z. Voloshina, M.Y. Antipina. *Russ. Chem. Bull. Int. Ed.*, **53**, 2097 (2004).
[23] Z. Biyiklioglu, E.T. Guner, H. Kantekin. *J. Incl. Phenom. Macrocycl. Chem.*, **60**, 235 (2008).
[24] H. Kantekin, A. Bakaray, Z. Bıyıklıoglu. *Transition Met. Chem.*, **32**, 209 (2007).
[25] E. Karapinar. *J. Incl. Phenom. Macrocycl. Chem.*, **53**, 171 (2005).
[26] A. Coskun, F. Yilmaz, E.G. Akgemci. *J. Incl. Phenom. Macrocycl. Chem.*, **60**, 393 (2008).
[27] H. Kantekin, A. Bakaray, Z. Bıyıklıoglu, M. Betul, K. Aslan. *Transition Met. Chem.*, **33**, 161 (2008).
[28] D. Sellmann, J. Utz, F.W. Heinemann. *Inorg. Chem.*, **38**, 459 (1999).
[29] M.C.M. Laranleira, R.A. Marusak, A.G. Lappin. *Inorg. Chim. Acta*, **300**, 186 (2000).
[30] K. Ohta, R. Higashi, M.I. Kejima, I. Yamamoto, N. Kobayashi. *J. Mater. Chem.*, **8**, 1979 (1998).
[31] S. Kumar, R. Singh, H. Singh. *J. Chem. Soc. Perkin Trans.*, **1**, 3049 (1992).
[32] G.N. Schrauzer, R.J. Windgassen. *J. Am. Chem. Soc.*, **88**, 3738 (1966).
[33] R.J. Henry. *Clinical Chemistry, Principles and Techniques*, 2nd Edn, p. 1393, Churchill Livingstone, New York (1974).
[34] S.C. Jackels, K. Farmery, E.K. Barefield, N.J. Rose, D.H. Busch. *Inorg. Chem.*, **11**, 2893 (1972).
[35] W.J. Geary. *Coord. Chem. Rev.*, **7**, 81 (1971).
[36] (a) N. Yamazaki, Y. Hohokabe. *Bull. Chem. Soc. Japan*, **44**, 63 (1971); (b) K. Dey, K. Mandal, M. Bandyopadhuay. *Indian J. Chem.*, **31A**, 937 (1992).
[37] S.C. Cummings, D.H. Busch. *Inorg. Chem.*, **10**, 1220 (1971).
[38] (a) L. Boucher, J.J. Katz. *J. Am. Chem. Soc.*, **89**, 1340 (1967); (b) H. Ogoshi, N. Masai, Z. Yoshida, J. Takemoto, K. Nakamoto. *Bull. Chem. Soc. Japan*, **44**, 49 (1971).
[39] M.M. Aly, A.O. Boghlaf, N.S. Gandji. *Polyhedron*, **4**, 1301 (1985).
[40] R. Blinc, D. Hadzi. *J. Chem. Soc.*, 4536 (1958).
[41] G.N. Schruzer. *Ber.*, **95**, 1438 (1962).
[42] K. Nakamoto. *Infrared and Raman Spectra of Inorganic and Coordination Compounds*, 3rd Edn, Wiley, New York (1977).
[43] J.R. Ferraro. *Low Frequency Vibrations of Inorganic and Coordination Compounds*, Plenum, New York (1971).
[44] (a) S. Buffagni, M.L. Vallarino, J.V. Quagliano. *Inorg. Chem.*, **3**, 671 (1964); (b) J.W.L. Martin, J.H. Timmons, A.E. Martel, P. Rudolf, A. Clearfield. *Inorg. Chem.*, **20**, 814 (1981).
[45] D.A. Waldwin, A.B.P. Lever, R.V. Parish. *Inorg. Chem.*, **10**, 107 (1971).
[46] B.K. Coltrain, S.C. Jackels. *Inorg. Chem.*, **20**, 2032 (1981).
[47] C.J. Ballhausen. *Introduction to Ligand Field Theory*, 1st Edn, Chap. 9, McGraw-Hill, USA (1962).
[48] R.A.D. Wentworth, T.S. Piper. *Inorg. Chem.*, **4**, 709 (1965).
[49] A.B.P. Lever. *Inorganic Electronic Spectroscopy*, 1st Edn, Chap. 9, Elsevier, Amsterdam (1968).
[50] (a) E. Ochiai, L.M. Long, C.R. Spats, D.H. Busch. *J. Am. Chem. Soc.*, **91**, 3201 (1969); (b) A.M. Tait, F.V. Lovecchio, D.H. Busch. *Inorg. Chem.*, **16**, 2206 (1977); (c) K.M. Long, D.H. Busch. *J. Coord. Chem.*, **4**, 113 (1974); (d) G.R. Brubaker, J.J. Fitzgerald. *J. Coord. Chem.*, **4**, 93 (1974); (e) Y. Hung, L.Y. Martin, S.C. Jackels, A.M. Tait, D.H. Busch. *J. Am. Chem. Soc.*, **99**, 4029 (1977).
[51] (a) R.A.D. Wentworth, T.S. Piper. *Inorg. Chem.*, **4**, 1524 (1965); (b) W.A. Baker, M.G. Phillips. *Inorg. Chem.*, **5**, 1042 (1966).
[52] K. Nakamoto, P.J. McCarthy. *Spectroscopy and Structure of Metal Chelate Complexes*, 1st Edn, Chap. 2, Wiley & Sons, USA (1968).
[53] R.J.P. Williams. *J. Mol. Catal.-Rev.*, **1**, 53 (1986).
[54] L. Vallee, R.J.P. Williams. *Proc. Natl Acad. Sci., USA*, **59**, 498 (1968).
[55] T. Hatakey, Z. Liu. *Handbook of Thermal Analysis*, Wiley, Chichester, UK (1998).
[56] G.H. Olive and S. Olive. *Coordination and Catalysis*, 1st Edn, Chap. 7, Verlag Chemie, Weinheim, New York (1977) and references therein.
[57] D.R. Armstrong, R. Fortune, P.G. Perkins. *Inorg. Chim. Acta*, **9**, 9 (1974).
[58] J.E. Huheey. *Inorganic Chemistry Principles of Structure and Reactivity*, 3rd Edn, Harper and Row, London (1983).
[59] A.M. Ramadan, R.M. Issa. *Transition Met. Chem.*, **30**, 471 (2005) and references therein.